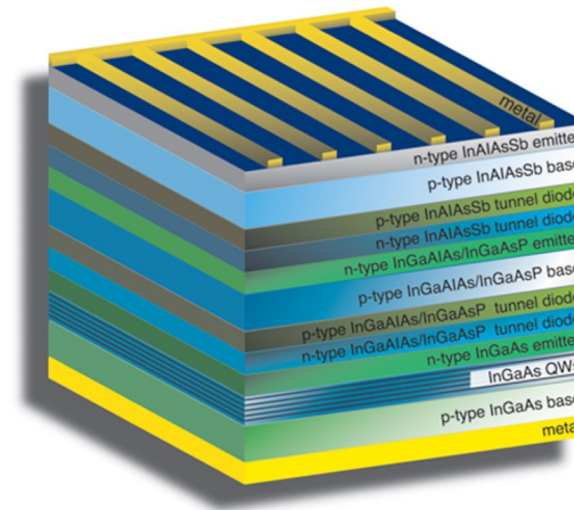


Lecture 10 – 19/11/2025

The p - n junction

- I - V characteristic: non ideal case
- Breakdown voltage
- Zener diode
- Avalanche diode
- Tunneling diode
- Solar cells



Summary Lecture 9

The p-n junction with gradient

$$V_{bi} = \frac{e\alpha W^3}{12\epsilon} \text{ and thus } W = \left(\frac{12\epsilon V_{bi}}{e\alpha} \right)^{1/3}$$

The p-n junction out of equilibrium

Potential drop: $\Delta V = V_{bi} - V$

Depletion region width:

$$W(V) = \sqrt{\frac{2\epsilon}{e} \left(\frac{N_A + N_D}{N_A N_D} \right) (V_{bi} - V)}$$

Quasi-Fermi levels:

*Non-degenerate

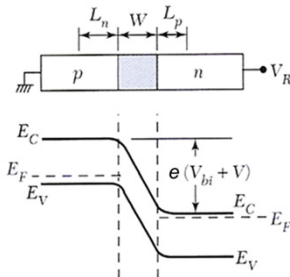
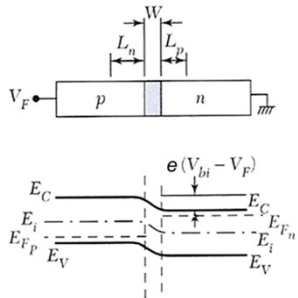
$$E_{F_n} = E_c - k_B T \ln \left(\frac{N_c}{n} \right) \text{ with } n = n_0 + G_n \tau_n \rightarrow \Delta n$$

$$E_{F_p} = E_v + k_B T \ln \left(\frac{N_v}{p} \right) \text{ with } p = p_0 + G_p \tau_p \rightarrow \Delta p$$

*Degenerate

$$E_{F_n} = E_c + \frac{\hbar^2}{2m_c^*} (3\pi^2 n)^{2/3}$$

$$E_{F_p} = E_v - \frac{\hbar^2}{2m_v^*} (3\pi^2 p)^{2/3}$$

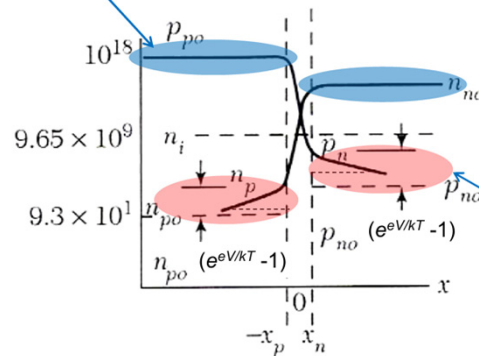


Minority carrier injection (Shockley)

Applying a voltage V changes the carriers' concentration at the depletion region boundaries (E field = 0).

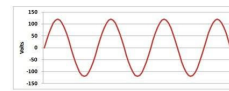
$$n_p - n_{p0} = n_{p0} \left(\exp \left\{ \frac{eV}{k_B T} \right\} - 1 \right) \text{ (on } p \text{ side boundary)}$$

$$p_n - p_{n0} = p_{n0} \left(\exp \left\{ \frac{eV}{k_B T} \right\} - 1 \right) \text{ (on } n \text{ side boundary)}$$



Rectifying behavior

Difference between forward ($\cong e^{eV/kT}, O(10^2 \text{ A})$) and reverse bias ($O(10^{-12} \text{ A})$) gives rise to a rectifying behavior.



I-V Characteristic

Continuity equation $D_n \frac{d^2 n_p}{dx^2} - \frac{n_p - n_{p0}}{\tau_n} = 0$, models how injected minority carriers diffuse.

Diffusion length $L_n = \sqrt{D_n \tau_n}$, before n_p recombines.

Diffusion currents from minority carriers

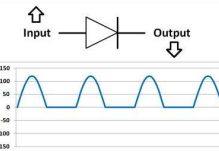
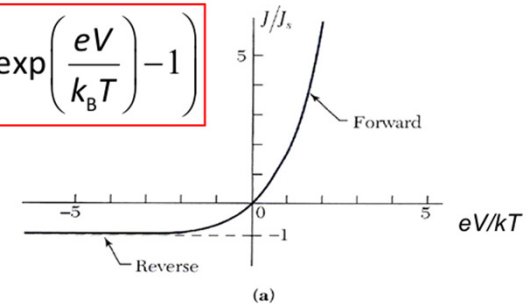
$$J_s = \frac{eD_n n_i^2}{N_A L_n} + \frac{eD_p n_i^2}{N_D L_p}$$

$$J = J_n(-x_p) + J_p(x_n)$$

$$= \frac{eD_n n_{p0}}{L_n} (e^{eV/k_B T} - 1) + \frac{eD_p p_{n0}}{L_p} (e^{eV/k_B T} - 1)$$

Small current density that flows under reverse bias

$$J(V) = J_s \left(\exp \left(\frac{eV}{k_B T} \right) - 1 \right)$$



I-V characteristic

The assumption we made regarding the absence of currents in the space charge region is quite rough.

Actually, there is often a non-negligible contribution to the current due to recombination and generation processes occurring in the depletion region (in Si and GaAs $p-n$ junctions because n_i is small, electron and hole emissions occur through bandgap generation-recombination centers located near the intrinsic Fermi level (e.g., Au and Cu in silicon and Cr in GaAs junctions))

Used for contacting

Used to get resistive layers

The total current density then writes

$$J = J_p + J_n + J_{r,g}$$

$$J \approx J_{p,diff} + J_{n,diff} + J_{r,g}$$

Under forward bias, the diffusion current dominates over the drift one!

I-V characteristic

Generation and recombination currents in the space charge region

$r > 0$ recombination rate
 $r < 0$ generation rate

$$r \approx \frac{1}{\tau} \frac{n_i^2 (e^{eV/k_B T} - 1)}{2n_i + p + n} \quad \text{and} \quad J_{g,r} = e \int_{-x_p}^{x_n} r dx$$

when $E_t = E_{Fi}$ **Cf. last Eq. slide #28 Lecture 7 and e-book by Sze**

1) Reverse bias: generation current

$-V \gg k_B T/e \Rightarrow r \approx -\frac{n_i}{2\tau_e}$ then

$$J_g = -\frac{en_i}{2\tau_e} W$$

Because n and $p \ll n_i$ in the reverse bias regime

Effective generation lifetime

$$W = \sqrt{\frac{2\epsilon}{e} \left(\frac{N_A + N_D}{N_A N_D} \right) (V_{bi} - V)}$$

$$eV_{bi} = E_g - k_B T \ln \left(\frac{N_V N_C}{N_A N_D} \right)$$

2) Forward bias: recombination current

Cf. Shockley's relations

r maximum for $n + p$ minimum (i.e., $n = p$) and $np = \text{cst} \Leftrightarrow n_n = p_n = n_i \exp(eV/2k_B T)$

$$r_{\max} = \frac{1}{\tau_e} \frac{n_i^2 (e^{eV/k_B T} - 1)}{2n_i (1 + e^{eV/2k_B T})}$$

$$V \gg k_B T/e \Rightarrow r_{\max} = \frac{n_i e^{eV/2k_B T}}{2\tau_e}$$

Effective recombination lifetime $\propto N_t^{-1}$

Finally,

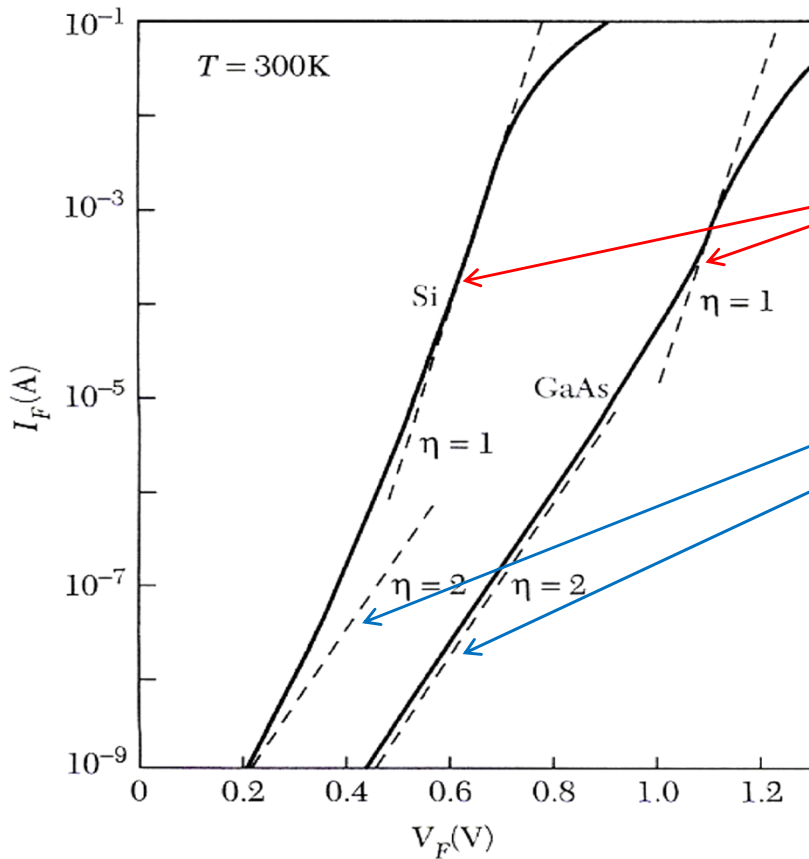
$$J_r = \frac{en_i}{2\tau_e} W_{\text{eff}}$$

with

$$W_{\text{eff}} = W e^{eV/2k_B T}$$

I-V characteristic

Experimental I-V curves



Total forward current density can be approximated, for $p_{n0} \gg n_{p0}$ (one-sided abrupt p^+n junction) and $V \geq 3k_B T/e$

$$J_F = e \sqrt{\frac{D_p}{\tau_p} \frac{n_i^2}{N_D}} e^{eV/k_B T} \frac{eWn_i}{2\tau_e} e^{eV/2k_B T}$$

$$\Rightarrow J_F \propto \exp\left(\frac{eV}{\eta k_B T}\right)$$

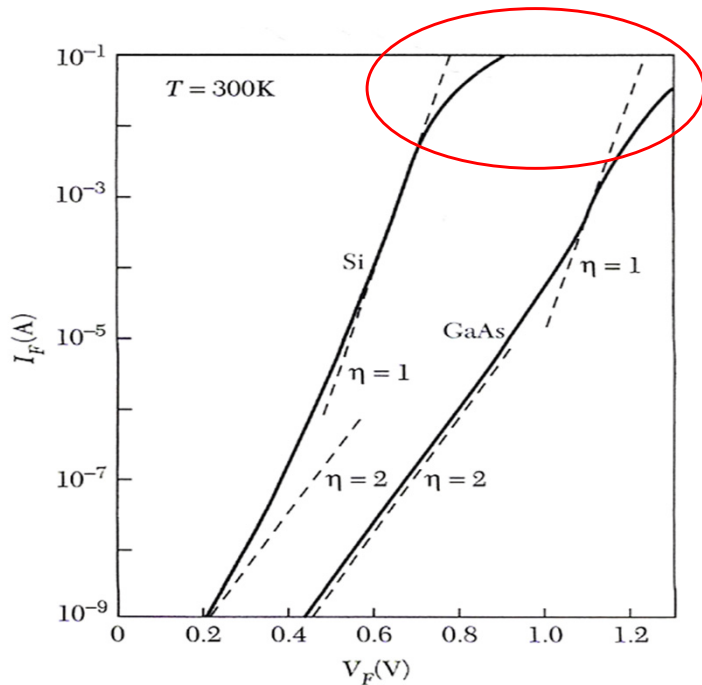
η ideality factor:

- $\eta = 1$ when ideal diffusion current dominates
- $\eta = 2$ when recombination current dominates

$$J(V) = J_s \left(\exp\left(\frac{eV}{\eta k_B T}\right) - 1 \right)$$

The ideality factor is a parametric function of the external bias, i.e., $\eta = \eta(V)$

I-V characteristic



Series resistance and high-injection

At high current levels, $\eta > 1$ and increases continuously with the forward voltage

1. Series resistance

Low and medium current levels: The potential drop IR_s across neutral regions remains small vs. $k_B T/e$ (silicon diode with $R_s = 1.5$ ohms, IR_s drop at 1 mA only 1.5 mV (vs. $k_B T/e$ of 26 mV at 300 K))

High current level: 100 mA, potential drop IR_s of 0.15 V (value six times larger than $k_B T/e$) \Rightarrow decrease of the bias across the depletion region

$$I \approx I_s e^{(e(V-R_s I))/\eta k_B T} = \frac{I_s e^{eV/\eta k_B T}}{e^{eR_s I/\eta k_B T}}$$

2. High-injection condition

$$p_n(x=x_n) \approx n_n \approx n_i \exp(eV/2k_B T) \text{ since } p_n n_n \approx p_{n0} n_{n0} e^{eV/k_B T} = n_i^2 \exp(eV/k_B T)$$

$$\Rightarrow I \propto \exp(eV/2k_B T)$$

Mass action's law extended to the out of equilibrium case (valid provided the semiconductor remains non-degenerated)

Specific p - n junctions: Zener, avalanche and tunneling diodes, solar cells

Reverse breakdown voltage

When the junction is reverse-biased (V_r), both the space charge region extent and the built-in electric field vary as $V_{\text{eff}}^{1/2}$ (where $V_{\text{eff}} = V_{\text{bi}} + V_r$),

Abrupt junction case

$$W = \sqrt{\frac{2\varepsilon}{e} \left(\frac{N_A + N_D}{N_A N_D} \right) V_{\text{eff}}} \quad E_{\text{max}} = 2V_{\text{eff}} / W \propto \sqrt{V_{\text{eff}}}$$

As a consequence, E_{max} increases but at a certain point:

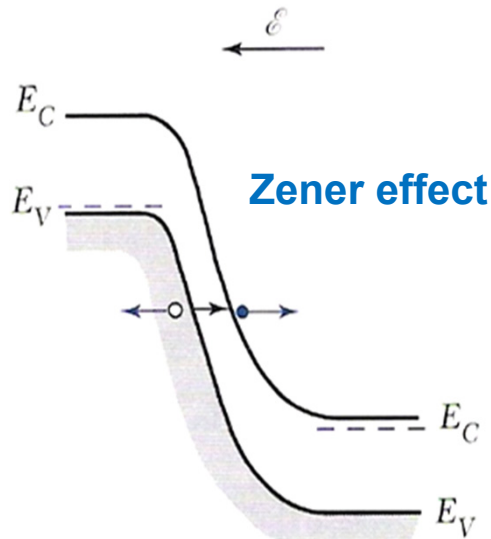
$F = qE_{\text{max}} \Rightarrow$ material/impact ionization leading to e-h pair generation

Silicon and GaAs: $E = 10^6$ V/cm or higher (breakdown voltage)

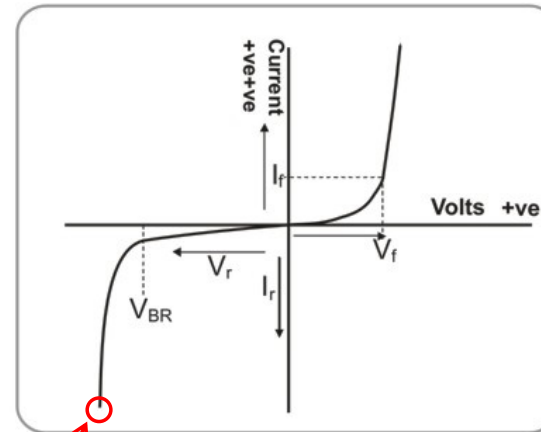
In a p - n junction this phenomenon limits the reverse bias called the **Zener voltage** (V_Z)

$V_r > V_Z \Rightarrow$ large current: **Zener** or junction breakdown occurs

Zener diode



N_A and $N_D > 5 \times 10^{17} \text{ cm}^{-3}$ in silicon and GaAs



$V_B < 4E_g/e \Rightarrow$ Zener or tunneling effect

$V_B > 6E_g/e \Rightarrow$ avalanche multiplication

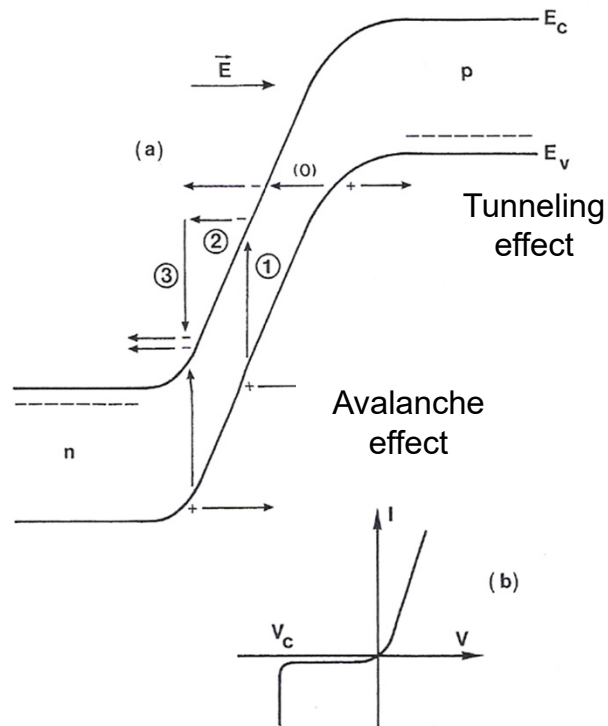
Intermediate voltages: mixture of tunneling and avalanche multiplication

A Zener diode relies on the tunneling effect: it occurs only in highly-doped p - n junctions

When the doping levels are “low” \Rightarrow “avalanche” effect

Process not inherently destructive but the maximum current must be limited by an external circuit to avoid any excessive junction heating

Avalanche diode



Avalanche effect

If the space charge region extent is large ($W > 0.1 \mu\text{m}$)
 \Rightarrow avalanche multiplication

For large reverse biases, e-h pairs are accelerated with a lot of energy, leading to breaking of lattice bonds upon collision with an atom which creates an e-h pair (*impact ionization*), newly created e-h pairs acquiring kinetic energy from the field, etc.

\Rightarrow *avalanche multiplication*

Case of asymmetric p - n junctions: p^+ - n one-sided abrupt junction with $N_D \leq 10^{17} \text{ cm}^{-3}$

Breakdown condition

I_{n0} : incident current on the left-hand side of the depletion region of width W with W large enough so as to initiate the avalanche multiplication process

I_n increases with the distance through the depletion region to reach the value $M_n I_{n0}$ at W
 M_n is the **multiplication factor** defined by $M_n = I_n(W)/I_{n0}$ (similar treatment for holes)

Total current $I = I_n + I_p$ (constant in the steady-state)

Incremental electron current at position x equals the number of e-h pairs generated per second over the distance dx :

$$d\left(\frac{I_n}{e}\right) = \left(\frac{I_n}{e}\right)(a_n dx) + \left(\frac{I_p}{e}\right)(a_p dx) \quad \text{with } a_n \text{ and } a_p \text{ the e-h ionization rates}$$

(a_n and $a_p \equiv$ number of e-h pairs generated by a free carrier per unit distance traveled)

$$\Rightarrow \frac{dI_n}{dx} - (a_n - a_p)I_n = a_p I$$

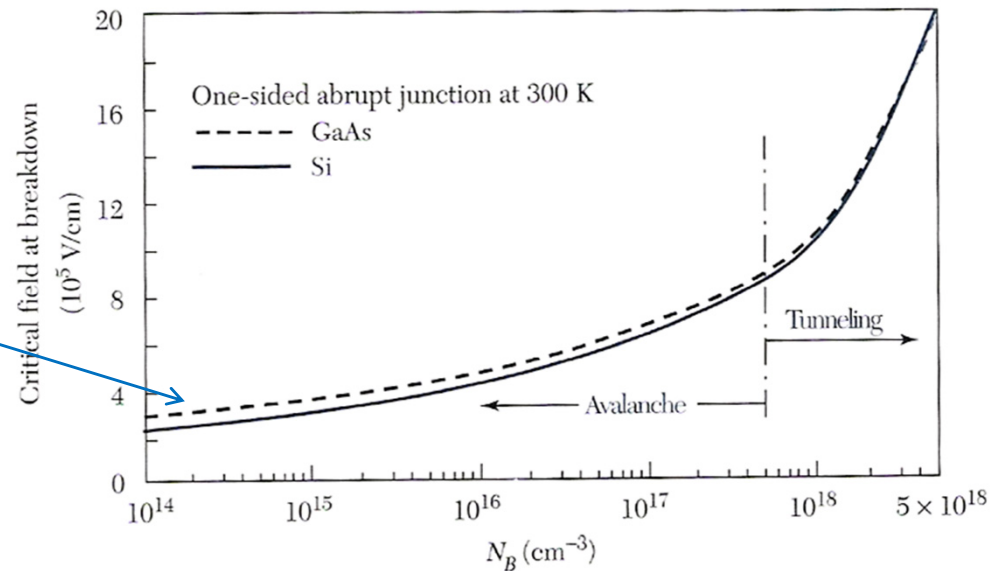
$$\text{If } a_n = a_p = a \Rightarrow \frac{I_n(W) - I_n(0)}{I} = \int_0^W a dx \Rightarrow 1 - \frac{1}{M_n} = \int_0^W a dx \quad (\text{assuming } I_n(W) = I), V_{B_{av}} \text{ obtained for } M_n \rightarrow \infty, \text{ i.e., } \int_0^W a dx = 1$$

Critical field at which the avalanche process occurs determined using measured a_n and a_p values + use of Poisson's equation:

$$V_{B_{av}} = \frac{WE_c}{2} = \frac{\epsilon_r \epsilon_0 E_c^2}{2e} (N_B)^{-1} \quad \begin{array}{l} E_c: \text{ critical field} \\ N_B: \text{ background doping lightly doped side} \end{array}$$

Critical field and breakdown voltage

Larger E_c and hence V_B value for GaAs due to larger bandgap vs Si as the avalanche process requires band-to-band excitations



Critical field at breakdown voltage for different background doping levels (N_B)

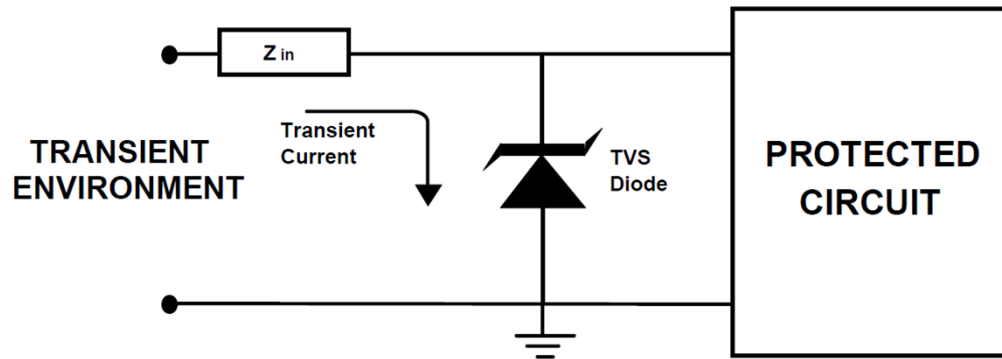
Approximate universal expression of V_B (abrupt junction):

$$V_B \approx 60(E_g/1.1)^{3/2} (N_B/10^{16})^{-3/4} \text{ V, with } E_g \text{ the room-temperature bandgap in eV and } N_B \text{ the background doping in } \text{cm}^{-3}$$

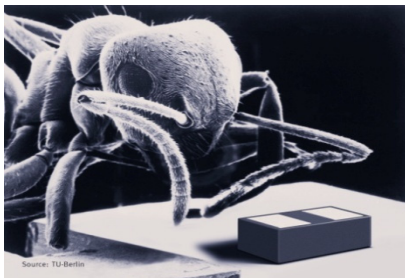
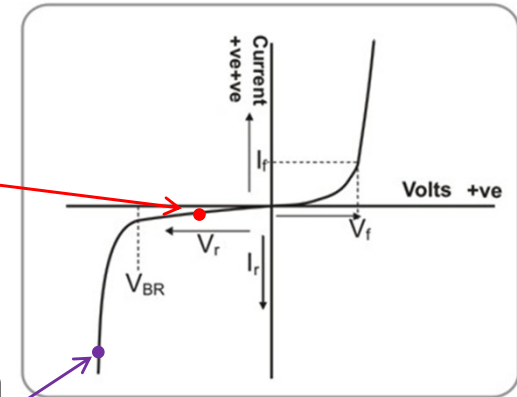
Avalanche multiplication mechanisms can generate microwave power (e.g., in IMPATT diodes) and detect optical signals as in an avalanche photodetector (high gain device used, e.g., for single photon detection)

Zener diode: electrostatic discharge damage protection

≡ parallel protection element for electrical components in case of voltage spikes



- High impedance under normal operating conditions
- Low impedance path for the transient current when the normal operating voltage of the protected circuit is exceeded

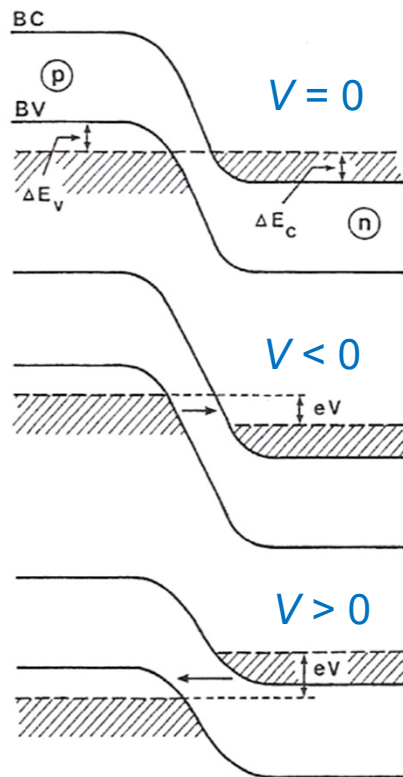


Infineon

The world smallest transient voltage suppression (TVS) diode for the protection of antennas comes from Infineon. With a footprint of just $0.62 \times 0.32 \text{ mm}^2$ in size and 0.31 mm in height (*it cannot be too small to act as an effective heat sink*)

Tunnel diode

n -type and p -type doped layers are degenerate (quasi-Fermi levels lie in the CB and VB)



High doping level $\Rightarrow W < 10$ nm

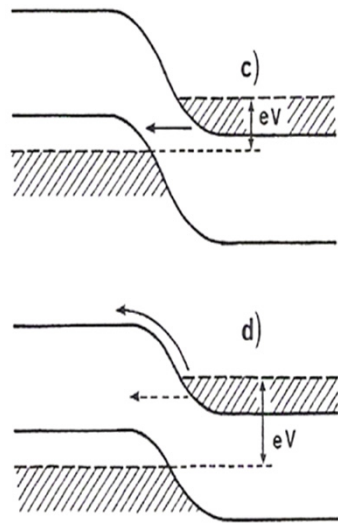
$V < 0$

Filled states in the VB have the same energy than the empty states in the CB \Rightarrow tunneling effect from the VB to the CB

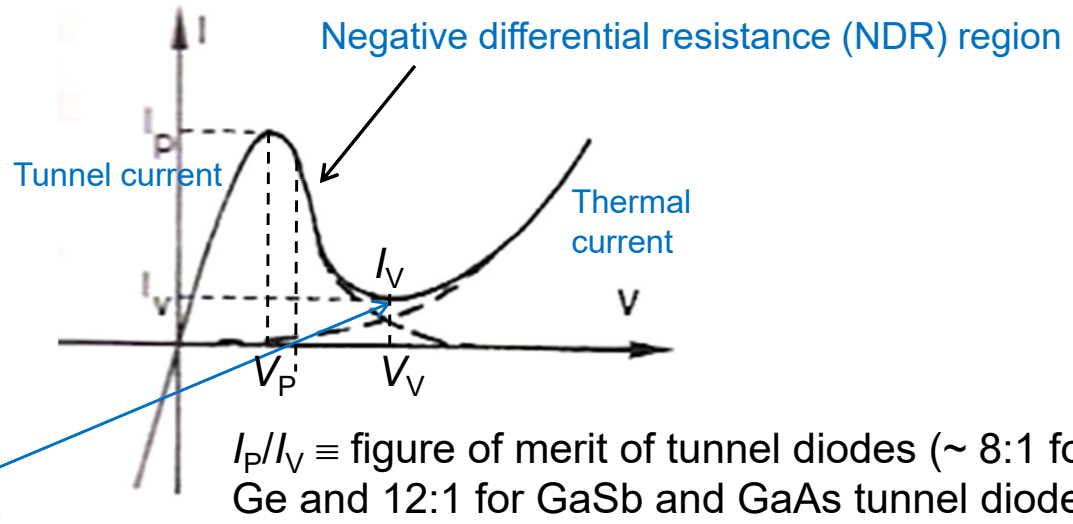
$V > 0$

tunneling effect from the CB to the VB

Tunnel diode



I minimum when $eV = \Delta E_V + \Delta E_C$



$I_P/I_V \equiv$ figure of merit of tunnel diodes ($\sim 8:1$ for Ge and $12:1$ for GaSb and GaAs tunnel diodes)

When such a diode is connected to an LC circuit (\equiv electrical resonator) at a DC bias voltage matching the NDR region, thermal noise induced oscillations in the microwave range can be generated

The tunnel diode was invented by Leo Esaki in 1958, Nobel prize in Physics in 1973

Tunnel diode

Very short tunneling time \Rightarrow use in the mm-wave region (devices with reduced parasitic capacitance and resistance, i.e., the RC time constant is small)

\rightarrow Time constant linked to cutoff frequency!

Low-power microwave applications: local oscillator, frequency-locking circuit

Transmission coefficient T of a particle through a 1D potential barrier of height eV_0 and thickness d :

$$T \propto \exp(-2\beta d) = \exp\left[-2d\sqrt{2m^*(eV_0 - E)/\hbar^2}\right]$$

See, e.g., Chap. 1 of *Quantum Mechanics Vol. 1* by Cohen-Tannoudji, Diu & Laloë (Wiley-VCH, Weinheim, 2020)

T value is finite if eV_0 , d and m^* are kept small!

I - V characteristic p^+ - n^+ junction

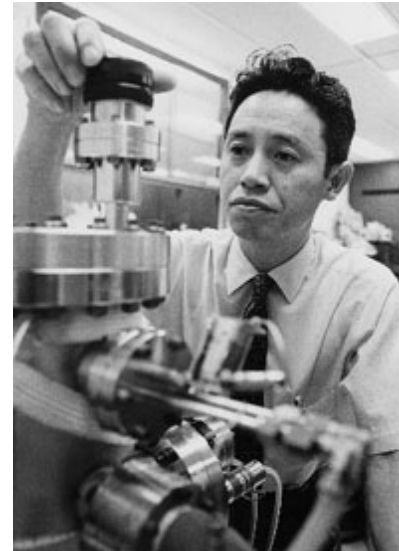
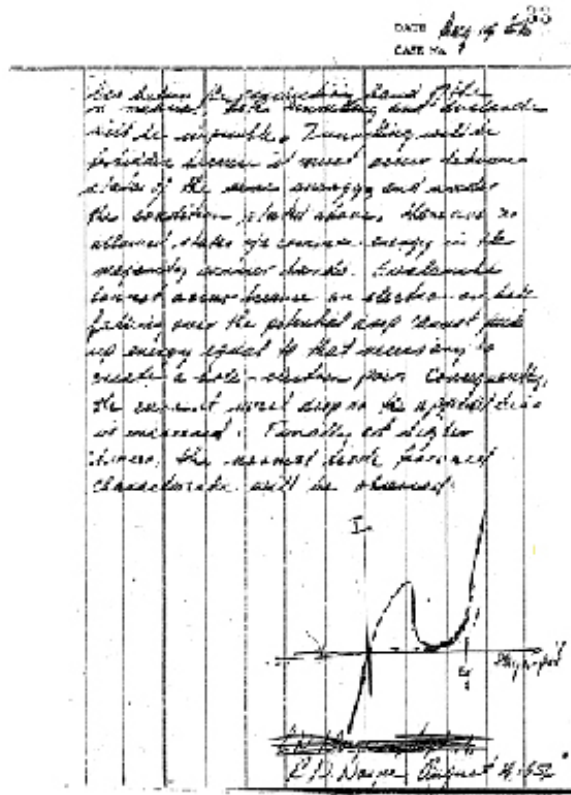
$$I = \underbrace{I_p \left(\frac{V}{V_p}\right) \exp\left(1 - \frac{V}{V_p}\right)}_{\text{Tunnel current}} + \underbrace{I_0 \exp\left(\frac{eV}{k_B T}\right)}_{\text{Thermal current}}$$

Negative differential resistance

$$R = \left(\frac{dI}{dV}\right)^{-1} = -\left[\left(\frac{V}{V_p} - 1\right) \frac{I_p}{V_p} \exp\left(1 - \frac{V}{V_p}\right)\right]^{-1}$$

Historical research article: L. Esaki, "New phenomenon in narrow germanium para-normal-junctions", Phys. Rev. **109**, 603 (1958) (> 1300 citations)

Tunnel diode



Dr. Leo Esaki joined IBM Research in 1960 and became an IBM Fellow in 1967. He was awarded the Nobel Prize in Physics in 1973 in recognition of his discovery of the tunnel diode.

Application of diodes: solar cells

Historical article: D. M. Chaplin, C. S. Fuller, and G. L. Pearson, "A new silicon p-n junction photocell for converting solar radiation into electrical power", J. Appl. Phys. **25**, 676 (1954) (> 1050 citations, 1-column long article)

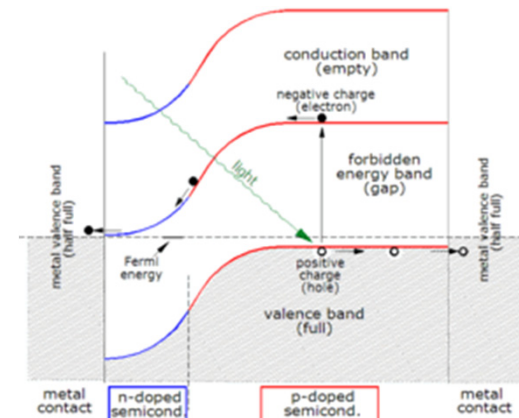
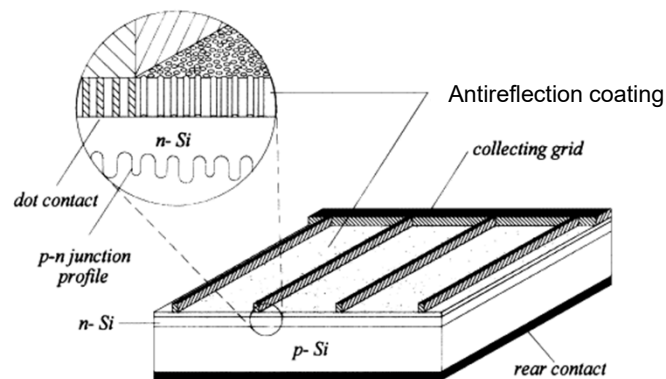
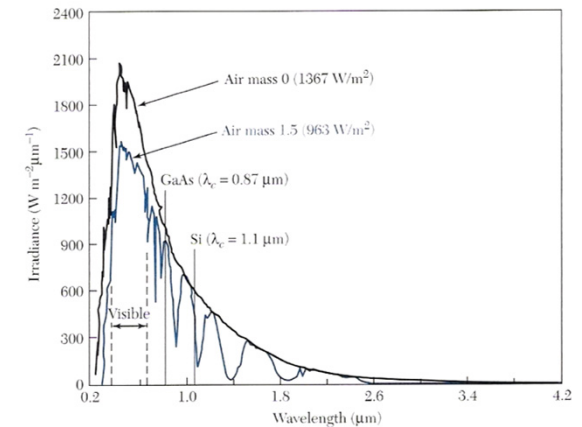
Intensity of solar radiation at average distance of Earth from the sun: 1367 W/m²

Atmosphere impact on sunlight: air mass (AM)

AM0: solar spectrum outside Earth's atmosphere (satellite, etc.)

AM1: sunlight at Earth's surface when the sun is overhead

Difference due to atmospheric attenuation (UV absorption in ozone, IR absorption in water vapor, scattering by airborne dust and aerosols)



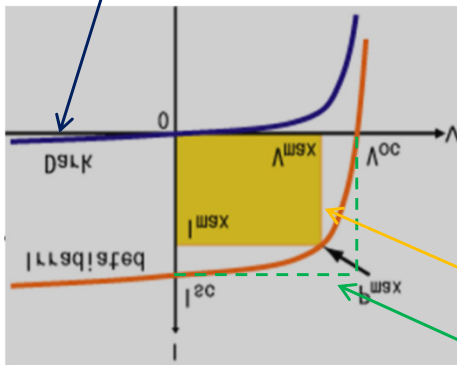
Application of diodes: solar cells

Ideal I - V characteristic of a solar cell under illumination:

$$I = I_s \left(e^{eV/k_B T} - 1 \right) - I_L \quad \text{with } I_L \text{ is the source current resulting from the excitation of excess carriers by solar radiation}$$

(R_L , load resistance)

$$\text{and } J_s = \frac{I_s}{A} = e N_C N_V \left(\frac{1}{N_A} \sqrt{\frac{D_n}{\tau_n}} + \frac{1}{N_D} \sqrt{\frac{D_p}{\tau_p}} \right) e^{-E_g/k_B T} \quad \text{with } A \text{ the device area}$$

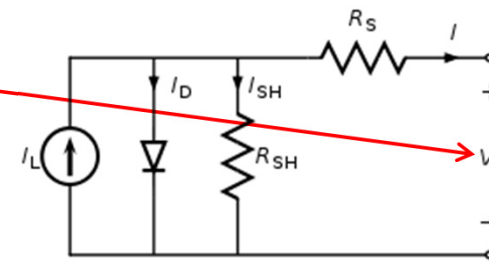


Inversion about the voltage axis!

With a proper load, close to 80% of the product $I_{sc} V_{oc}$ can be extracted (with $I_{sc} = I_L$)

Conversion efficiency (case of a perfect solar cell, no series resistance R_s , etc.)

$$\eta = \frac{I_{\max} V_{\max}}{P_{\text{in}}} = \frac{FF \cdot I_L V_{oc}}{P_{\text{in}}} \quad \text{where } P_{\text{in}} \text{ is the incident power and } FF \text{ the fill factor defined as } FF \equiv \frac{I_{\max} V_{\max}}{I_L V_{oc}}$$



$$V_{oc} (I = 0) = \frac{k_B T}{e} \ln \left(\frac{I_L}{I_s} + 1 \right) \approx \frac{k_B T}{e} \ln \left(\frac{I_L}{I_s} \right)$$

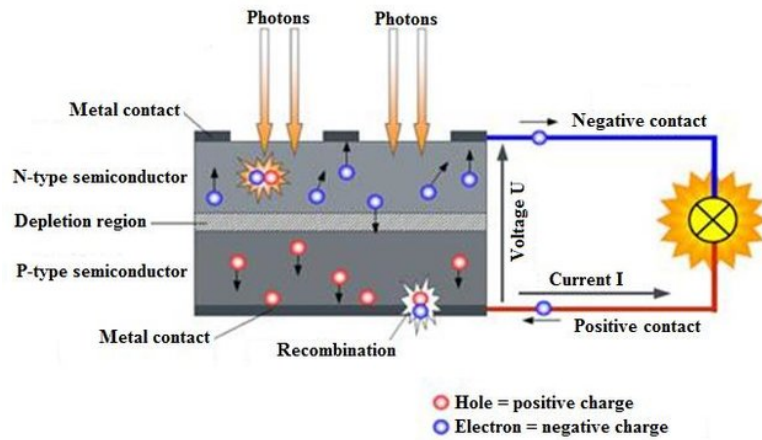
$$P = IV = I_s V \left(e^{eV/k_B T} - 1 \right) - I_L V$$

Maximum power when $dP/dV = 0$,

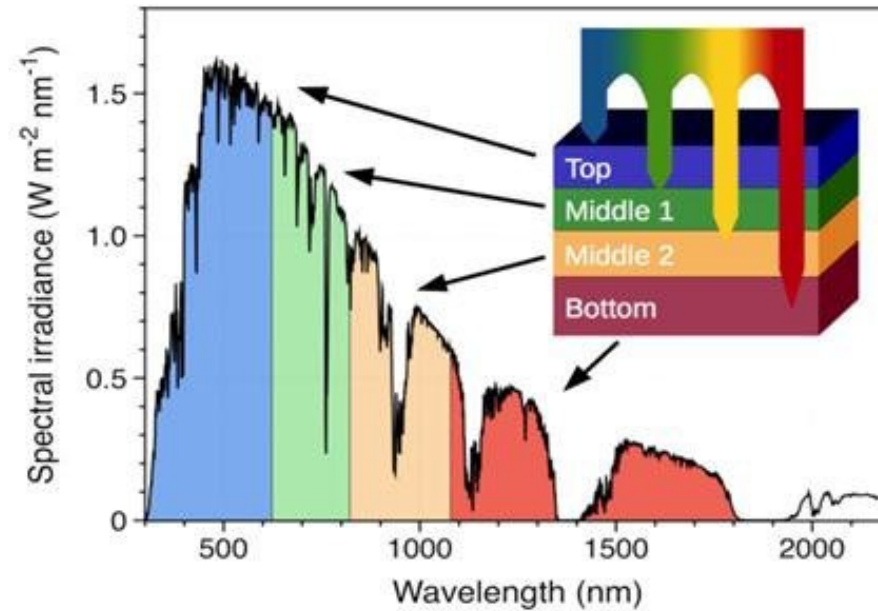
$$P_{\max} = I_{\max} V_{\max} \approx I_L \left[V_{oc} - \frac{k_B T}{e} \ln \left(1 + \frac{eV_{\max}}{k_B T} \right) - \frac{k_B T}{e} \right]$$

Latest fill factor values of 87.5% for a single junction Si solar cell with $\eta \approx 27.8\%$ (G. Wang *et al.*, Nature **647**, 369 (2025))

Application of diodes: multi-spectral solar cells

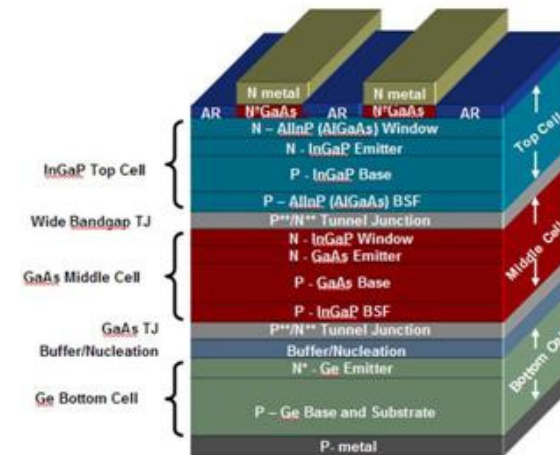
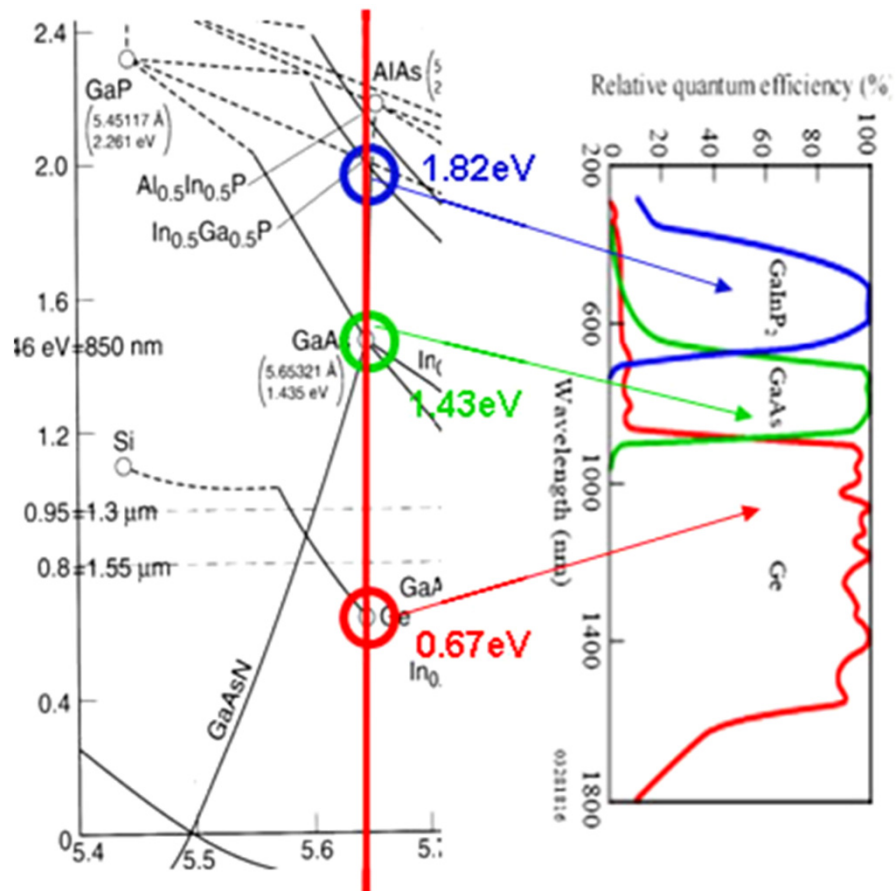


Different solar cells in series to cover the whole solar spectrum



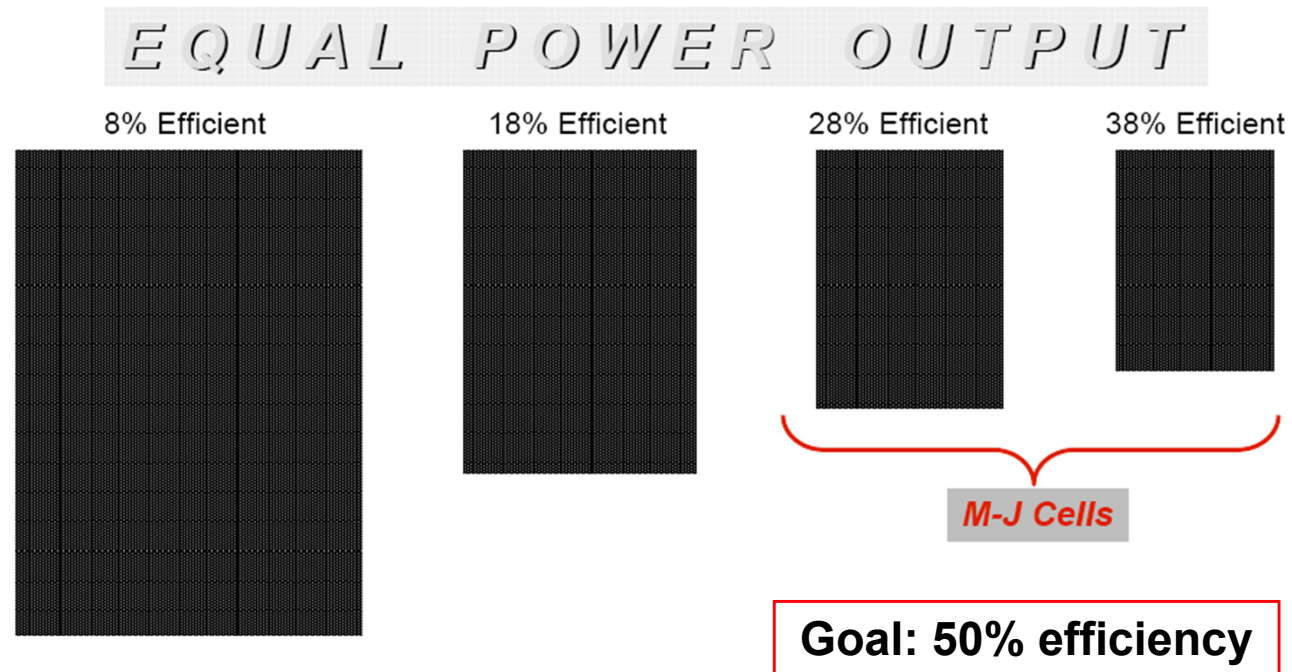
Higher solar cell efficiency

Multi-spectral solar cells



Multi-spectral solar cells

Solar Cell Efficiency makes a big difference in the size and cost of the photovoltaic element

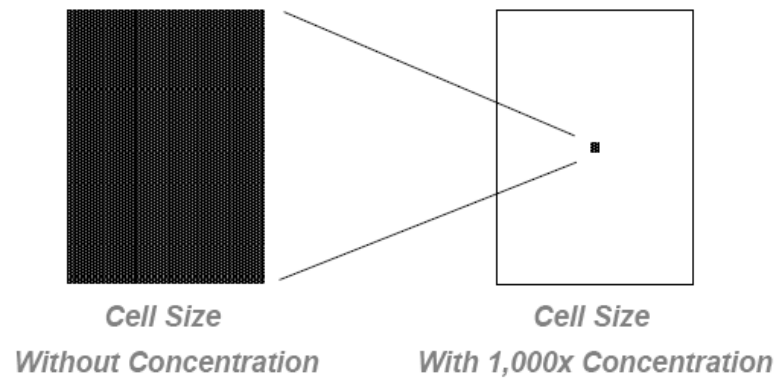


2022: 39.5% - NREL

Solar cells with concentrator

Concentration enables the use of very small solar cells

EQUAL POWER OUTPUT



2023: 47.6% - Fraunhofer Institute for Solar Energy Systems

Solar cells

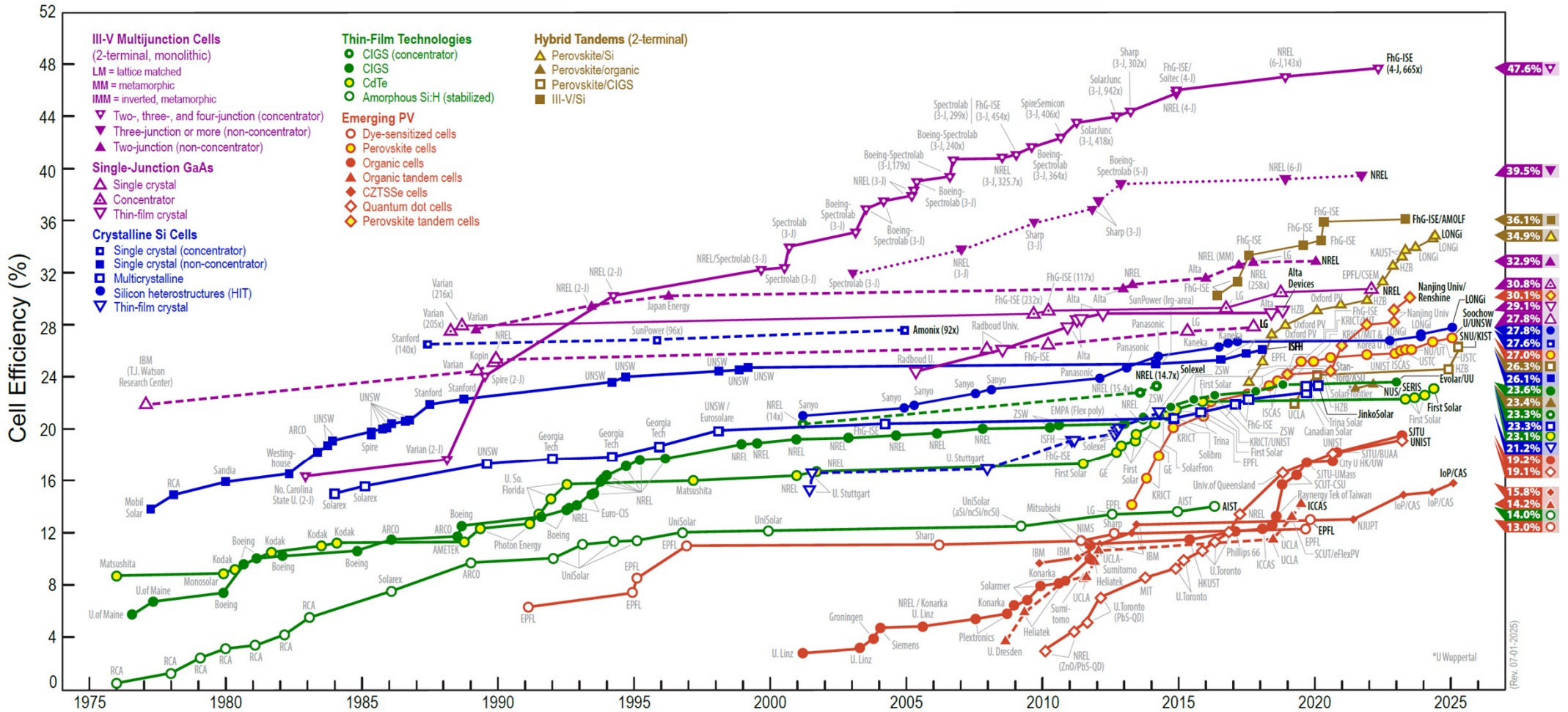
- **Improved cell efficiency**
 - More power from the same area
- **Optimized optics**
 - Reduce lost sunlight
- **Low cost components**
 - Structural members can be manufactured in low cost countries
- **Heliostat**
 - All of the above with fewer, simpler moving parts



- Current cost (2020) in the USA: \$0.05-0.13/kWh
@ \$0.05/kWh, a 6 kW residential system will resume to \$1.4 per Watt
- Current cost (2019) in the EU: €0.052/kWh
⇒ Mostly due to decrease in the cost of PV modules

Solar cell efficiency (2025 update)

Best Research-Cell Efficiencies

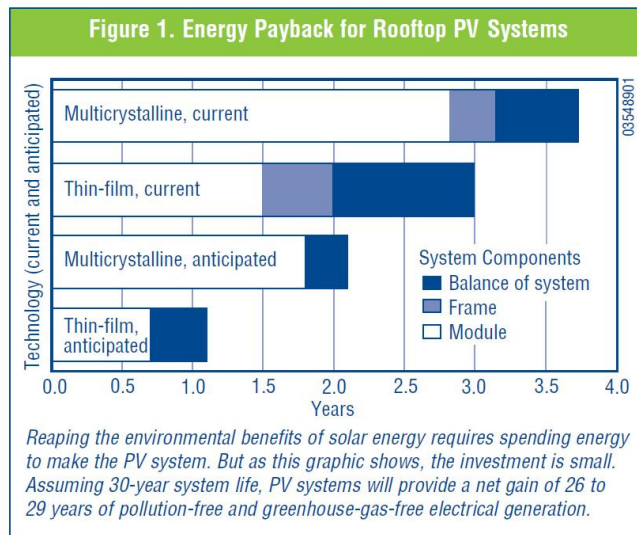


CIGS: copper indium gallium selenide
 Semiconductor physics and light-matter interaction

Key research article: W. Shockley and H. J. Queisser, "Detailed balance limit of efficiency of p-n junction solar cells", J. Appl. Phys. **32**, 510 (1961) (> 11000 citations)

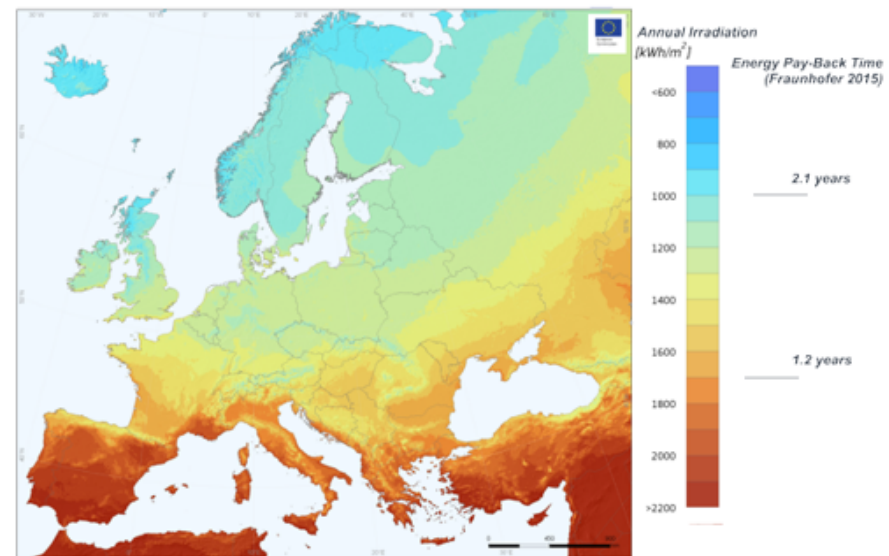
Solar cells: payback for PV systems

Multicrystalline silicon PV rooftop modules



Source: DOE/NREL

Photovoltaic Solar Electricity Potential in European Countries



Source: Fraunhofer ISE